



Published in final edited form as:

Nature. 2010 December 2; 468(7324): 705–708. doi:10.1038/nature09546.

## Structural Changes of Envelope Proteins During Alphavirus Fusion

Long Li, Joyce Jose, Ye Xiang, Richard J. Kuhn, and Michael G. Rossmann

Department of Biological Sciences, Purdue University, 915 W. State Street, West Lafayette, IN 47907-2054, USA

### Abstract

Alphaviruses are enveloped RNA viruses that have a diameter of about 700 Å and can be lethal human pathogens<sup>1</sup> (Fig. 1). Entry of virus into host cells by endocytosis is controlled by two envelope glycoproteins, E1 and E2. The E2-E1 heterodimers form 80 trimeric spikes on the icosahedral virus surface<sup>1,2</sup>, 60 with quasi-threefold symmetry and 20 coincident with the icosahedral threefold axes arranged with T=4 quasi-symmetry (Fig. 1a). The E1 glycoprotein has a hydrophobic fusion loop at one end and is responsible for membrane fusion<sup>3,4</sup>. The E2 protein is responsible for receptor binding<sup>5,6</sup> and protects the fusion loop at neutral pH. The lower pH in the endosome induces the virions to undergo an irreversible conformational change in which E2 and E1 dissociate and E1 forms homotrimers, triggering fusion of the viral membrane with the endosomal membrane and then releasing the viral genome into the cytoplasm<sup>3,4</sup>. Here we report the structure of an alphavirus spike, crystallized at low pH, representing an intermediate in the fusion process and clarifying the maturation process. The trimer of E2-E1 in the crystal structure is similar to the spikes in the neutral pH virus except that the E2 middle region is disordered, exposing the fusion loop. The amino- and carboxy-terminal domains of E2 each form immunoglobulin-like folds, consistent with the receptor attachment properties of E2.

---

The X-ray crystal structure of the ectodomain of the E1 protein (residues 1-383) from Semliki Forest virus (SFV) is homologous to the flavivirus E glycoprotein and consists of three  $\beta$ -barrel domains (DI, DII and DIII) with the fusion loop at the distal end of DII<sup>7</sup>. The structure of the E1 ectodomain had been fitted into the 9 Å resolution cryo-EM reconstruction of Sindbis virus, generating a partial structure of the virus<sup>8,9</sup>. After subtraction of the density representing E1, the E2 density was found to be a long, thin

---

Users may view, print, copy, download and text and data-mine the content in such documents, for the purposes of academic research, subject always to the full Conditions of use: [http://www.nature.com/authors/editorial\\_policies/license.html#terms](http://www.nature.com/authors/editorial_policies/license.html#terms)

Correspondence should be addressed to M.G.R. (mr@purdue.edu).

**Author Contributions** LL designed the expression constructs, JJ cloned the constructs, and LL & JJ developed the expression system and purified the protein. LL crystallized the protein, collected X-ray diffraction data and, with YX, determined the structure. LL, RJK and MGR discussed the results and wrote the paper.

**Author Information** The atomic coordinates of the E2-E1 heterodimer crystal structures have been deposited with the Protein Data Bank (accession numbers 3MUU). The fit of the E2-E1 heterodimer into the cryoEM reconstruction of Sindbis virus has been deposited with the Protein Data Bank (accession number 3MUW).

**Supplementary Information** accompanies the paper on [www.nature.com/nature](http://www.nature.com/nature).

The authors have no competing financial interests which might influence the results or interpretation given in this manuscript.

volume that covers the top of each E1 molecule including the fusion loop<sup>8</sup>. However, the crystal structure of E2 has remained unknown until now.

An E2-E1 recombinant protein of Sindbis virus, in which the ectodomains of E2 and E1 were connected by a flexible Strep-tag linker<sup>10</sup> (Fig. 1b & S1), was expressed in *Drosophila* S2 cells. The size exclusion chromatography showed that the purified protein existed in solution as trimers of the E2-E1 heterodimer over a pH range from 5.5 to 9.5. The protein was crystallized at pH 5.6, which is lower than the pH 6.0 fusion threshold for alphaviruses<sup>4,11,12</sup>. The resultant crystal structure consisted of trimers of E2-E1 heterodimers that were remarkably similar to the trimeric spikes in the virus (Fig. 2 & Table S1), demonstrating the biological significance of the crystallized recombinant E2-E1 protein.

The C $\alpha$  backbone of E2 corresponded well with an earlier tracing obtained by connecting known markers such as glycosylation and antibody binding sites<sup>8</sup> (Fig. 3). The structure of E2 consists of the amino terminal domain A (residues 1 to 132), the middle domain B and the carboxy-terminal domain C (residues 264 to 343). The ~88 residues of domain B are mostly disordered and are connected to domains A and C by long connecting linker peptides (the “ $\beta$ -ribbon connector”). The connecting peptide from domain A to domain B starts at residue 133 and could be traced to residue 166. The connecting peptide from domain B to domain C picks up at residue 255 and continues to residue 263 where it enters domain C (Fig. S2). The three domains of E2 are stretched out along the length of E1 in the order C, A and B, with C being closest to the viral membrane and mostly hidden from the viral exterior. Domain B, had it not been disordered, would correspond to the tip of the cryo-EM envelope (Fig. 3b). The glue between the three E1 molecules that constitute a spike is formed by E2 domain C, which binds to DII in adjacent E1 molecules within the trimeric spike (Figs. 2c & S3a). The residues in the contact area are primarily hydrophilic making a number of potential hydrogen bonds (Table S2.1). In contrast to the low pH, partially disordered structure described here, the fully ordered structure of E2 has been determined at neutral pH for Chikungunya virus in the accompanying paper<sup>15</sup>.

Both domain A and domain C have the topology of an immunoglobulin fold (Fig. 3). This is consistent with E2 functioning as a cell receptor binding protein. Furthermore, residues that had been identified in E2 to be associated with altered receptor binding and tropism are now seen to be in domain A of E2 (Table S3, Fig. S4). However, other residues that were associated with cell recognition<sup>6,13,14</sup> are in the disordered domain B showing that there could be multiple sites on the virus surface that associate with various cell surface molecules involved in virus attachment and entry.

The A domains of the three E2 molecules within one trimeric spike are situated in the center of the triangular cavity formed by the three E1 molecules in the spike and make extensive interactions with each other (Table S2.2). The presence of histidines, arginines and lysines in the interface, although not conserved among alphaviruses, shows that the interactions will become weak or repulsive as the pH drops below the pK of the histidines. Furthermore, the extensive positive charge on these surfaces suggests that the A domains might be easily

separated and then alter their orientation to present their arginines and lysines to the phospholipid headgroups in the membrane.

If the envelope of the E2 density derived from the 9 Å resolution cryo-EM map<sup>8</sup> is overlaid onto the E2-E1 trimeric low pH crystal structure by superimposing the E1 molecules, then a large proportion of the tip of the E2 cryo-EM envelope, presumably corresponding to the B domain, overlaps and clashes with a neighboring trimeric spike assembly in the crystal structure (Fig. S5a). This is shown even more dramatically by superimposing the neutral pH crystal structure of the Chikungunya virus E2-E1 heterodimer as found in the accompanying paper<sup>15</sup> (Fig. S5b) onto the low pH crystal structure reported in this paper. (The rms deviation between C $\alpha$  atoms in the ordered part of E2 in these two structures is 4.5 Å, a reasonable result considering that only 36% of the residues are identical in the compared region.) Thus, domain B as found in the virus cannot be in the same position in the crystal structure, partly consistent with the findings of Wu *et al.*<sup>16</sup>. The  $\beta$ -ribbon connector peptides that extend from domains A and C follow the edge of domain A and are within the E2 envelope observed in the cryoEM map. Thus, the “disorder” of domain B (which is stabilized by two disulphide bonds<sup>15</sup>) might be because the long  $\beta$ -ribbon connector is flexible and allows domain B to detach itself from the tip of E2. The  $\beta$ -ribbon connector is flanked by two completely conserved histidines at Sindbis positions 169 and 256. These might be the acid sensitive triggers that perhaps control the interaction with E3 (see below) and cause the  $\beta$ -ribbon connector to dissociate itself from the A domain. In summary, whereas the position of domain B in the neutral pH virus covers the fusion loop on E1, protecting the virus from premature fusion with other cellular membranes, acidification of the virus causes domain B to move away from its neutral pH position, thereby exposing the fusion loop and making it accessible to lipid membranes (Fig. 4). Antibodies that bind to epitopes on domain A or B are strong neutralizers<sup>17</sup>, perhaps because these antibodies might prevent not only receptor attachment but also prevent disordering of domain B and, hence, inhibit fusion,

During maturation E1 and PE2 (the precursor to the E3-E2 proteins before cleavage of E3, also referred to as p62) are assembled as heterodimers in the endoplasmic reticulum<sup>1,18</sup> and processed through the Golgi and trans-Golgi network (TGN) where E3 protects the E2-E1 heterodimer from premature fusion with cellular membranes. The resultant E2-E1 heterodimers, or E3-E2-E1 in some viruses<sup>19</sup>, are then transported to the plasma membrane<sup>20</sup> where budding occurs following association of the glycoproteins with preformed nucleocapsids.

The site of E3 has been mapped by various cryo-EM studies<sup>21-23</sup> that can now be identified as corresponding to a site where domain A borders onto domain B (Figs. S3b and 4). This suggests that the function of E3 is to stabilize the  $\beta$ -ribbon connector. As long as the distal end of the  $\beta$ -ribbon connector remains associated with domain A and DII, domain B will continue to protect the fusion loop. This is supported by mutational studies of H169 in Sindbis virus and its equivalent residue in Semliki Forest virus<sup>24,25</sup>.

Fusion of the viral membrane with the cellular plasma membrane in alphaviruses requires the dissociation of the E1-E2 heterodimer and formation of E1 homotrimers at low pH<sup>26</sup> in

the presence of a lipid membrane. In the E1 homotrimeric structure the E1 molecules are arranged with their long direction running roughly parallel to a common threefold axis of rotation, exposing the fusion loops of each monomer at one end of the trimeric complex<sup>27</sup>. Residues of E1 that were in contact with E2 in the pre-fusion trimeric spike (in part determined from the structure given in the accompanying paper<sup>15</sup>) are located on the surface of the post-fusion E1 homotrimer, facing away from the spike axes, and are predominantly in surface loops<sup>8</sup> (Fig. S6). The conformational changes required to form a post-fusion trimer will require the removal of the E2 molecules from the center of the trimeric spike to the outside and rotation of the E1 molecules by about 180° about their long axes to face each other across what was the threefold axis of the pre-fusion spike. E2 might escape the embrace of the surrounding E1 molecules by detaching the C domains and slipping to the outside via the gap left by the C domains. Alternatively, two E1 molecules on neighboring spikes might combine with a third E1 molecule recruited from another unmatched E1 molecule elsewhere on the virus to make the post-fusion trimer (Fig. 4). Similar, huge conformational changes occur in the maturation and fusion of flaviviruses<sup>28,29</sup>, leaving the question “What is the pathway by which these events happen?”.

## Methods Summary

The recombinant E2-E1 protein was expressed in a *Drosophila* expression system. The protein was purified by His-tag affinity, ion exchange and size exclusion chromatography. A crystallization robot and 96-well sitting drop plates were used for the initial crystallization screening. The one condition that grew crystals was subsequently optimized using hanging drops with 24-well plates. The crystal diffraction data were collected at the Advanced Photon Source synchrotron. The crystal structure was determined by combining the SeMet multiple wavelength anomalous dispersion (MAD) and molecular replacement methods. The crystal structure was fitted into the electron microscopy image reconstruction density of Sindbis virus using the program EMfit<sup>30</sup>.

**Full Methods** and any associated references are available in the online version of the paper at [www.nature.com/nature](http://www.nature.com/nature).

## Methods

### Protein production

The coding sequences of E3 (residues 1-64), E2 (residues 1-344) and E1 (residues 1-384) of Sindbis virus (Toto64) were amplified by PCR<sup>31</sup>. The DNA sequence of a peptide linker, STREP, that contains the Strep-tag II<sup>10</sup> (GGGSWSHPQFEKGGGG) was inserted between E2 and E1 by overlapping PCR, thereby omitting the trans-membrane and 6K region between E2 and E1. The recombinant gene that codes for E3-E2 (residues 1-344)-STREP-E1 (residues 1-384) was inserted between the Bgl II and Xho I restriction sites in the pMT/BiP/V5-His A vector (Invitrogen Corp.). A (His)<sub>6</sub> tag and a stop codon was introduced right after the 3' end of the E1 gene by the 3' PCR primer, so the V5 and the His tags from the original vector were omitted from the expression product. Ten µg of the resultant plasmid were co-transfected with 0.5 µg of the plasmid pCoHygro (Invitrogen Corp.) into 3 ml of *Drosophila* S2 cells at 2-4×10<sup>6</sup> cells/ml by using 30 µl of Cellfectin (Invitrogen Corp.)

in Schneider's *Drosophila* medium (no serum) (Invitrogen Corp.). The stable cell line expressing the recombinant protein was selected out after one month in the presence of 300 µg/ml Hygromycin B (EMD Chemicals Inc.) in Schneider's *Drosophila* medium supplemented with 10% heat inactivated fetal bovine serum. Stably transfected cells were gradually scaled up and adapted into EX-CELL 420 serum-free medium (Sigma-Aldrich Co.). Protein expression was induced by addition of 500 µM CuSO<sub>4</sub> after 2 L of the cells, maintained in two 3 L spinner flasks, had grown to a density of 6-10×10<sup>6</sup> cells/ml. The recombinant protein was secreted into the medium as the E2-E1 complex since E3 was cleaved by furin and the furin-like proteases during secretion in the S2 cells. The medium was harvested 3-5 days post induction. The cells were spun down and the supernatant medium was collected and clarified by passing through 0.22 µm cutoff membrane filters (Millipore Corp.). The medium was then loaded onto a column packed with 18 ml IMAC sepharose 6 ff resin (GE Healthcare), pre-charged with Ni<sup>2+</sup> [32]. The protein was eluted with 100 and then 500 mM imidazole using a step elution protocol. The partially purified protein was dialyzed against a phosphate buffer (20 mM NaPO<sub>4</sub>, 50 mM NaCl, pH 6.9) at 4°C overnight. The dialyzed protein solution was loaded onto a 1 ml Hitrap Q and then onto a 1 ml Hitrap SP column (GE Healthcare). The protein was eluted from the SP column with a 50-500 mM NaCl gradient. Solubility of the protein was 1-2 mg/ml in neutral and low pH buffers. However, the protein could be concentrated to 5-10 mg/ml when the pH of the buffer was raised to 9.5 or higher. Thus, the protein solution was dialyzed against a CHES buffer (20 mM CHES, 100 mM NaCl, pH 9.5) and the protein was purified by passing through a gel filtration column (Superdex 200, GE Healthcare). The purified protein was concentrated to 4-5 mg/ml in the CHES buffer for crystallization.

To produce the selenomethionine (SeMet)-substituted protein, the medium was replaced with ESF 921 serum-free methionine-free medium (Expression Systems, LLC) after 2 L of cells had reached a concentration of 10-12×10<sup>6</sup> cells/ml. The cells were starved for 4-6 hours before 400 mg/L L-SeMet (Acros Organics) and 500 µM CuSO<sub>4</sub> were added. The medium was harvested 2-3 days after induction. The purification was similar to that of the native protein. Amino acid analysis showed that 90% of native methionine in the protein had been substituted by SeMet.

### Crystallization and diffraction data collection

Crystals of the native E2-E1 protein grew at 20 °C by using the hanging drop method. 1.5 µl of the protein solution and 1.5 µl of the mother solution were mixed and hung over 500 µl of the mother solution containing 11% polyethylene glycol (PEG) 8000, 200-275 mM Na/K Tartrate, 0.1M Na/KPO<sub>4</sub> pH 5.6. Crystals of the SeMet protein grew with the mother solution containing 9-10% PEG 8000, 300-375 mM Na/K Tartrate, 0.1 M Na/KPO<sub>4</sub> pH 5.6. The crystals appeared in three days and grew to full sizes in 2-4 weeks. The crystals were soaked in the mother liquid plus 20% PEG 400 as a cryo-solvent, followed by flash-freezing in liquid nitrogen. Hundreds of crystals were screened at the Advanced Photon Source (APS, Argonne National Laboratory, USA). The limits of the diffraction were gradually improved from 8 Å to 4 Å resolution. In general, the SeMet protein crystals diffracted better than the native protein crystals. The first complete data set of a native crystal extended to only 4 Å resolution. The best data sets were obtained from the SeMet protein crystals pre-treated with

the mother liquid plus 20% PEG 400 and 1% H<sub>2</sub>O<sub>2</sub> for 60 sec before freezing<sup>33</sup>. A multi-wavelength anomalous diffraction (MAD) data set with a resolution limit of 3.3 Å was collected at the APS beamline 23 ID-B (Table S1).

### Structure determination

The data were processed using the HKL2000 program<sup>34</sup>. The output intensity files were converted to structure factor files for the CCP4 program package<sup>35</sup>. For the first native data with the resolution of 4 Å, the space group was determined to be P321 with one E2-E1 heterodimer in an asymmetric unit. The pre- and post-fusion structures of the Semliki Forest virus E1 protein (Protein Data Bank accession number 2ALA and 1RER) were used to generate search models for molecular replacement using the program Phaser<sup>36</sup>. A solution was found when domains I and II (DI-II) from the pre-fusion E1 structure were used as a search model. However, the quality of the resultant electron density map was not good enough to interpret the E2 molecule. A single wavelength anomalous dispersion (SAD) data set of a SeMet crystal was collected with a resolution of 3.7 Å and space group P321. Ten out of the 11 selenium (Se) sites in the protein were found by using the program SHELXD<sup>37</sup>. Later, a three-wavelength MAD data set was collected with the peak wavelength data having the resolution of 3.3 Å. The space group was determined to be P1 with six E2-E1 heterodimers in an asymmetric unit and cell dimensions similar to the P321 space group. The crystallographic 3, 2 and 2<sub>1</sub> axes present in the P321 space group were now only approximate non-crystallographic symmetry (NCS) axes indicating that the overall molecular packing remained similar to that of the P321 space group. The initial Se sites were generated by using all the Se sites in one unit cell of the SAD data collected for the space group P321. The sites were refined in the program SHARP<sup>38</sup>. The quality of the resultant map was greatly improved by sixfold NCS averaging and other density improvement methods implemented in the programs DM<sup>39</sup> and RESOLVE<sup>40</sup>. DI-II of E1 and domains A and C of E2 could be traced in the density map. A barrel-shape density was evident for each of the six independent DIII domains of E1, although the individual chains could not be traced. Therefore, the DIII model of Semliki Forest virus was placed in the density using a real space search procedure with the program ESSENS<sup>41</sup>, followed by rigid body refinement with the program REFMAC5<sup>42</sup>. The E2-E1 model was built by using the program COOT<sup>43</sup> with the guidance from the (2F<sub>o</sub> - F<sub>c</sub>), (F<sub>o</sub> - F<sub>c</sub>), omit, and B-factor sharpened (2F<sub>o</sub>-F<sub>c</sub>) maps. Structure refinement was performed by using the programs PHENIX<sup>44</sup> and REFMAC5<sup>42</sup> with tight NCS restraints and TLS refinement<sup>45</sup> (Fig. S7, Table S1). The electron density for DIII was recognizable, but the mean B factor of the main chain atoms of DIII was 270 Å<sup>2</sup> as opposed to 120 Å<sup>2</sup> for the main chain atoms in DI and DII. The structure of E2, lying roughly parallel to E1 was as expected. Each spike structure consisted of a three-start right-handed helix with a maximum diameter of about 78 Å.

The crystallographic 32 symmetry in the trigonal space group (or quasi-32 symmetry in the triclinic space group) produced two twofold-related trimers of E2-E1 heterodimers. In the triclinic cell the crystallographic three- and twofold axes were only approximate because of a slight rotation and displacement of each of the two spikes in the unit cell. Superposition of the crystal structure onto the cryo-EM structure<sup>8</sup> gave a rms deviation of 3.4 Å between equivalent Ca atoms in D1 and D2.



## Fitting of the crystal structure into the cryo-EM density of the virus

The crystal structure of the E2-E1 heterodimer was fitted into the 9 Å resolution cryo-EM map of Sindbis virus<sup>8</sup> (Electron Microscopy Data Bank Accession code 1121) using the program EMfit<sup>46</sup>, and gave a fit that was at least as good as the independent fitting of three SFV structures of E1 into the Sindbis virus cryo-EM density<sup>8</sup>. DI-II and DIII of E1, domain A, the β-ribbon connector and domain C of E2 were fitted as individual rigid bodies for each of the four quasi-equivalent positions (Table S4).

The DI-DII component of E1 had behaved as a rigid body in previous structural analyses of alphavirus particles<sup>8,9</sup>, but the angle between DIII and DI-DII was found to be variable. In the crystal structure reported here the angle between DI-DII and DIII has changed by about 9° relative to the angles observed in the neutral pH cryo-EM structure of Sindbis virus or 18° relative to the crystal structure of SFV E1.

Domain A was found to be rotated (~10°) and translated (~5Å) slightly relative to the crystal structure in order to obtain the best fit into the cryo-EM density. This small conformational change of the A domain within the trimeric spike may be the result of crystal packing where a carbohydrate moiety associated with Asn318 in E2 interacts with domain A in a neighboring spike. As the structure of the B domain has two disulphide bonds (Voss *et al.*, accompanying paper)<sup>15</sup>, it is likely to be a rigid body. Attempts were made, using the computer program EMfit<sup>46</sup> to determine alternative positions of the B domain in the uninterpreted regions of density tentatively interpreted as solvent. A number of likely positions were found that had the N- and C-termini of domain B within 20 Å of the C and N discontinued ends of the β-ribbon connector, respectively.

Figures displaying the structure were generated with the program Chimera<sup>47</sup>.

## Supplementary Material

Refer to Web version on PubMed Central for supplementary material.

## Acknowledgments

We wish to thank Siyang Sun, Anastasia Aksyuk, and Thomas Edwards for many helpful discussions. We are also grateful to Sheryl Kelly for help in the preparation of the manuscript. We thank Felix Rey for sharing the coordinates of Chikungunya virus E2-E1 to help interpret the Sindbis virus cryoEM density of the E2 domain B. We would like to thank the staff at the Advanced Photon Source, Argonne National Laboratory, GM/CA sector for their help in data collection. The work was supported by NIH Grants to RJK and MGR.

## References

1. Strauss JH, Strauss EG. The alphaviruses: gene expression, replication, and evolution. *Microbiol. Rev.* 1994; 58:491–562. [PubMed: 7968923]
2. von Bonsdorff CH, Harrison SC. Sindbis virus glycoproteins form a regular icosahedral surface lattice. *J. Virol.* 1975; 16:141–145. [PubMed: 48559]
3. Kielian M. Membrane fusion and the alphavirus life cycle. *Adv. Virus Res.* 1995; 45:113–151. [PubMed: 7793323]
4. White J, Helenius A. pH-dependent fusion between the Semliki Forest virus membrane and liposomes. *Proc. Natl. Acad. Sci. U.S.A.* 1980; 77:3273–3277. [PubMed: 6997876]

5. Dubuisson J, Rice CM. Sindbis virus attachment: isolation and characterization of mutants with impaired binding to vertebrate cells. *J. Virol.* 1993; 67:3363–3374. [PubMed: 7684466]
6. Strauss EG, Stec DS, Schmaljohn AL, Strauss JH. Identification of antigenically important domains in the glycoproteins of Sindbis virus by analysis of antibody escape variants. *J. Virol.* 1991; 65:4654–4664. [PubMed: 1714515]
7. Lescar J, et al. The fusion glycoprotein shell of Semliki Forest Virus: an icosahedral assembly primed for fusogenic activation at endosomal pH. *Cell.* 2001; 105:137–148. [PubMed: 11301009]
8. Mukhopadhyay S, et al. Mapping the structure and function of the E1 and E2 glycoproteins in alphaviruses. *Structure.* 2006; 14:63–73. [PubMed: 16407066]
9. Zhang W, et al. Placement of the structural proteins in Sindbis virus. *J. Virol.* 2002; 76:11645–11658. [PubMed: 12388725]
10. Schmidt TG, Skerra A. The Strep-tag system for one-step purification and high-affinity detection or capturing of proteins. *Nat. Protoc.* 2007; 2:1528–1535. [PubMed: 17571060]
11. Smit JM, Bittman R, Wilschut J. Low-pH-dependent fusion of Sindbis virus with receptor-free cholesterol- and sphingolipid-containing liposomes. *J. Virol.* 1999; 73:8476–8484. [PubMed: 10482600]
12. White J, Kartenbeck J, Helenius A. Fusion of Semliki Forest virus with the plasma membrane can be induced by low pH. *J. Cell Biol.* 1980; 87:264–272. [PubMed: 7419594]
13. Meyer WJ, Johnston RE. Structural rearrangement of infecting Sindbis virions at the cell surface: mapping of newly accessible epitopes. *J. Virol.* 1993; 67:5117–5125. [PubMed: 7688818]
14. Zhang W, Heil M, Kuhn RJ, Baker TS. Heparin binding sites on Ross River virus revealed by electron cryo-microscopy. *Virology.* 2005; 332:511–518. [PubMed: 15680416]
15. Voss JE, et al. Crystal structures of the immature and mature surface glycoprotein complexes of Chikungunya virus. *Nature.* 2010 co-submission.
16. Wu S-R, et al. The dynamic envelope of a fusion class II virus. Prefusion stages of Semliki Forest virus revealed by electron cryomicroscopy. *J. Biol. Chem.* 2007; 282:6752–6762. [PubMed: 17192272]
17. Griffin DE. Roles and Reactivities of Antibodies to Alphaviruses. *Semin. Virol.* 1995; 6:249–255.
18. Wahlberg JM, Boere WA, Garoff H. The heterodimeric association between the membrane proteins of Semliki Forest virus changes its sensitivity to low pH during virus maturation. *J. Virol.* 1989; 63:4991–4997. [PubMed: 2479769]
19. Ziemiecki A, Garoff H. Subunit composition of the membrane glycoprotein complex of Semliki Forest virus. *J. Mol. Biol.* 1978; 122:259–269. [PubMed: 691044]
20. Ziemiecki A, Garoff H, Simons K. Formation of the Semliki Forest virus membrane glycoprotein complexes in the infected cell. *J. Gen. Virol.* 1980; 50:111–123. [PubMed: 7441208]
21. Ferlenghi I, et al. The first step: activation of the Semliki Forest virus spike protein precursor causes a localized conformational change in the trimeric spike. *J. Mol. Biol.* 1998; 283:71–81. [PubMed: 9761674]
22. Paredes AM, et al. Structural localization of the E3 glycoprotein in attenuated Sindbis virus mutants. *J. Virol.* 1998; 72:1534–1541. [PubMed: 9445057]
23. Wu SR, Haag L, Sjoberg M, Garoff H, Hammar L. The dynamic envelope of a fusion class II virus. E3 domain of glycoprotein E2 precursor in Semliki Forest virus provides a unique contact with the fusion protein E1. *J. Biol. Chem.* 2008; 283:26452–26460. [PubMed: 18596032]
24. Zhang X, Kielian M. Mutations that promote furin-independent growth of Semliki Forest virus affect p62-E1 interactions and membrane fusion. *Virology.* 2004; 327:287–296. [PubMed: 15351216]
25. Heidner HW, McKnight KL, Davis NL, Johnston RE. Lethality of PE2 incorporation into Sindbis virus can be suppressed by second-site mutations in E3 and E2. *J. Virol.* 1994; 68:2683–2692. [PubMed: 7908062]
26. Wahlberg JM, Garoff H. Membrane fusion process of Semliki Forest virus. I. Low pH-induced rearrangement in spike protein quaternary structure precedes virus penetration into cells. *J. Cell Biol.* 1992; 116:339–348. [PubMed: 1370493]



27. Gibbons DL, et al. Conformational change and protein-protein interactions of the fusion protein of Semliki Forest virus. *Nature (London)*. 2004; 427:320–325. [PubMed: 14737160]
28. Li L, et al. The flavivirus precursor membrane-envelope protein complex: structure and maturation. *Science*. 2008; 319:1830–1834. [PubMed: 18369147]
29. Yu IM, et al. Structure of the immature dengue virus at low pH primes proteolytic maturation. *Science*. 2008; 319:1834–1837. [PubMed: 18369148]
30. Rossmann MG, Bernal R, Pletnev SV. Combining electron microscopic with X-ray crystallographic structures. *J. Struct. Biol.* 2001; 136:190–200. [PubMed: 12051899]
31. Owen KE, Kuhn RJ. Identification of a region in the Sindbis virus nucleocapsid protein that is involved in specificity of RNA encapsidation. *J. Virol.* 1996; 70:2757–2763. [PubMed: 8627749]
32. Lehr RV, Elefante LC, Kikly KK, O'Brien SP, Kirkpatrick RB. A modified metal-ion affinity chromatography procedure for the purification of histidine-tagged recombinant proteins expressed in *Drosophila* S2 cells. *Protein Expr. Purif.* 2000; 19:362–368. [PubMed: 10910726]
33. Sharff AJ, Koronakis E, Luisi B, Koronakis V. Oxidation of selenomethionine: some MADness in the method! *Acta Crystallogr. sect. D.* 2000; 56:785–788. [PubMed: 10818365]
34. Otwinowski Z, Minor W. Processing of X-ray diffraction data collected in oscillation mode. *Meth. Enzymol.* 1997; 276:307–326.
35. Collaborative Computational Project Number 4. The CCP4 suite: programs for protein crystallography. *Acta Crystallogr. sect. D.* 1994; 50:760–763. [PubMed: 15299374]
36. McCoy AJ, et al. Phaser crystallographic software. *J. Appl. Cryst.* 2007; 40:658–674. [PubMed: 19461840]
37. Sheldrick GM. A short history of SHELX. *Acta Crystallogr. sect. A.* 2008; 64:112–122. [PubMed: 18156677]
38. de La Fortelle E, Bricogne G. Maximum-likelihood heavy-atom parameter refinement for multiple isomorphous replacement and multiwavelength anomalous diffraction methods. *Meth. Enzymol.* 1997; 276:472–494.
39. Cowtan KD. 'dm': an automated procedure for phase improvement by density modification. *Joint CCP4 and ESF-EACBM Newsletter on Protein Crystallography.* 1994; 31:34–38.
40. Terwilliger TC. Maximum-likelihood density modification. *Acta Crystallogr. sect. D.* 2000; 56:965–972. [PubMed: 10944333]
41. Kleywegt GJ, Jones TA. Template convolution to enhance or detect structural features in macromolecular electron-density maps. *Acta Crystallogr. sect. D.* 1997; 53:179–185. [PubMed: 15299952]
42. Murshudov GN, Vagin AA, Dodson EJ. Refinement of macromolecular structures by the maximum-likelihood method. *Acta Crystallogr. sect. D.* 1997; 53:240–255. [PubMed: 15299926]
43. Emsley P, Cowtan K. Coot: model-building tools for molecular graphics. *Acta Crystallogr. sect. D.* 2004; 60:2126–2132. [PubMed: 15572765]
44. Adams PD, et al. PHENIX: a comprehensive Python-based system for macromolecular structure solution. *Acta Crystallogr. D Biol. Crystallogr.* 2010; 66:213–221. [PubMed: 20124702]
45. Winn MD, Isupov MN, Murshudov GN. Use of TLS parameters to model anisotropic displacements in macromolecular refinement. *Acta Crystallogr. sect. D.* 2001; 57:122–133. [PubMed: 11134934]
46. Rossmann MG, Bernal R, Pletnev SV. Combining electron microscopic with X-ray crystallographic structures. *J. Struct. Biol.* 2001; 136:190–200. [PubMed: 12051899]
47. Pettersen EF, et al. UCSF Chimera—a visualization system for exploratory research and analysis. *J. Computat. Chem.* 2004; 25:1605–1612.

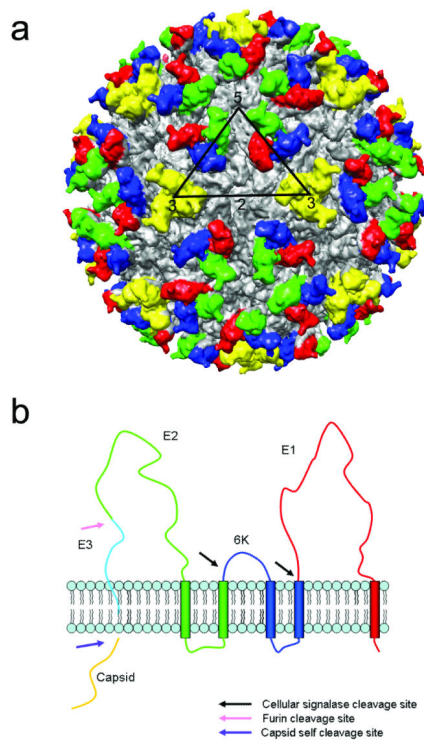


**Figure 1.**

The structural proteins of an alphavirus. a, The cryo-EM density of Sindbis virus showing  $T=4$  symmetry. The four E2 molecules in one asymmetric unit (outlined in black) are colored red, green, blue and yellow. These give rise to one trimeric spike on each icosahedral threefold axis and one generally positioned spike. The E1 molecules are colored grey. b, Threading of the Sindbis virus structural polyprotein through an endoplasmic reticulum membrane showing the position of the capsid, E3, E2, 6K and E1 proteins.

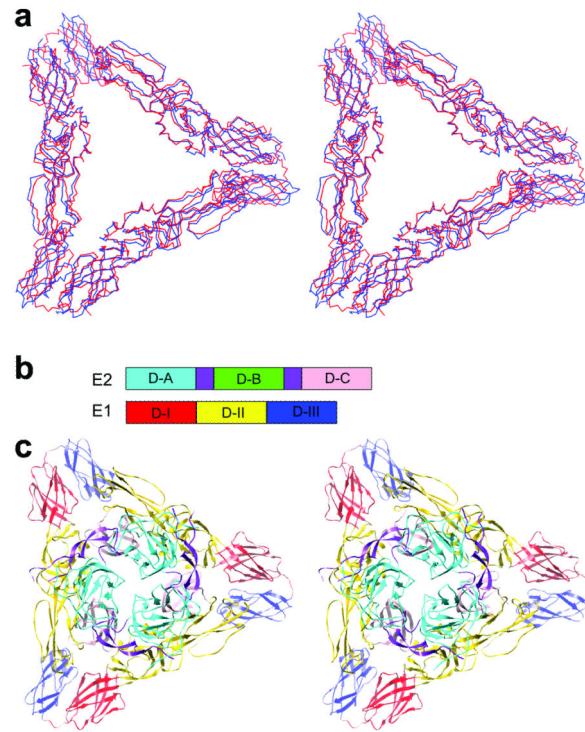


**Figure 2.**

Stereo diagrams showing the trimeric spike structure. a, The E1 molecule in a Sindbis virus spike (blue) compared with the E1 molecules in the crystal structure (red) b, linear representation of polypeptides showing domains D-A (cyan), D-B (green), D-C (pink) and the  $\beta$ -ribbon connector (purple) in E2; as well as the domains DI (red), DII (yellow), and DIII (blue) in E1. c, Crystal structure of the trimeric spike at low pH. Domain B is disordered.

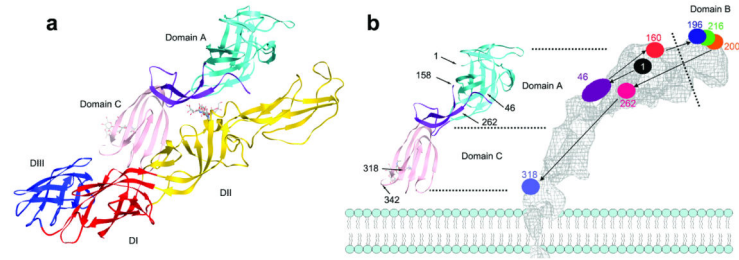


**Figure 3.**

The E2-E1 heterodimer. a, The crystal structure (left) color coded as in Fig. 2b. b, Comparison of the earlier E2 mapping<sup>8</sup> with the E2 crystal structure. Amino acid sequence numbers are given in strategic positions<sup>8</sup>. The lipid envelope is shown diagrammatically. [Reprinted from Mukhopadhyay, S. et al. Mapping the structure and function of the E1 and E2 glycoproteins in alphaviruses. *Structure* 14, 63-73, (2006).]

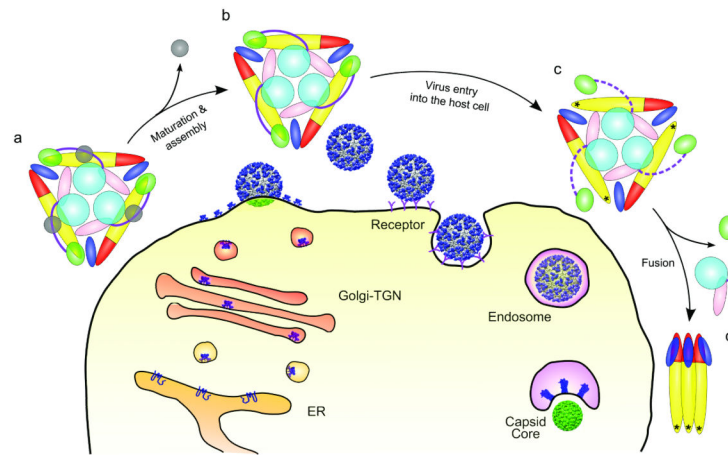


**Figure 4.**

Cartoon showing maturation and fusion. Color-coded as in Fig. 2b. a, The viral spike while being transported through the Golgi and TGN. Domain B is attached to domain II because E3 (grey) binds the  $\beta$ -ribbon connector to domain A and holds E2 in place at low pH. b, The viral spike on the virus after E3 has been proteolytically cleaved and, in Sindbis virus, has been jettisoned. c, After the virus has recognized a host cell and entered into a low pH endosomal vesicle, domain B becomes unattached from DII, exposing the fusion loop (marked with an \*). The dashed line indicates the disordered  $\beta$ -ribbon connector. d, The trimeric spike disassembles, allowing escape of E2 and formation of E1 homotrimers.